Sharper Insights: CMOS Cameras Enhance BeamSquared

Written by: PhD Mark Ivker, Senior Physicist at Ophir Optronics, Sneha Patil Application Engineer at Ophir Optronics, Karol Sanilevitch, Senior R&D engineer at Ophir Optronics

Starting in 2024, the MKS Ophir BeamSquared analyzer will be equipped with the new SP204S backside illuminated CMOS camera. This camera has several advantages over the older CCD camera (SP920) it is replacing. CMOS cameras lack the smearing found in CCD cameras. Our latest cameras also show a greatly reduced blooming effect particularly attributed to CMOS sensors. Backside illuminated CMOS sensors flip and thin the silicon, enhancing photodiode light collection efficiency for improved sensitivity. The new camera combined with our advanced BeamSquared system brings in improvement in sensitivity and M² measurement in the NIR region. The reduced pixel size in the new camera allows measurement of smaller beam sizes accurately.

Why CMOs is better than CCD technology?

Both CCD and CMOS sensors absorb light in similar semiconductor heterojunction structures (usually a pinned photodiode), CCDs must transport the photoexcited charges from pixel to pixel and finally to the edge of the active region where they are converted to a voltage and then digitized to give the reading. In the CMOS architecture, each pixel has its own transistors for converting the generated electrons into a voltage and amplifying it. The voltages are sequentially sampled by analog to digital circuits at the edge of the active area to produce the digital readout signal. By sampling voltage instead of transporting charge, CMOS cameras solve the problem of smearing which appears in CCD cameras close to saturation. Smearing also occurs in the CCD farther from saturation for light in the near infrared (NIR), above 1000 nm. See an example of CCD smearing in figures 1 and 2 below.
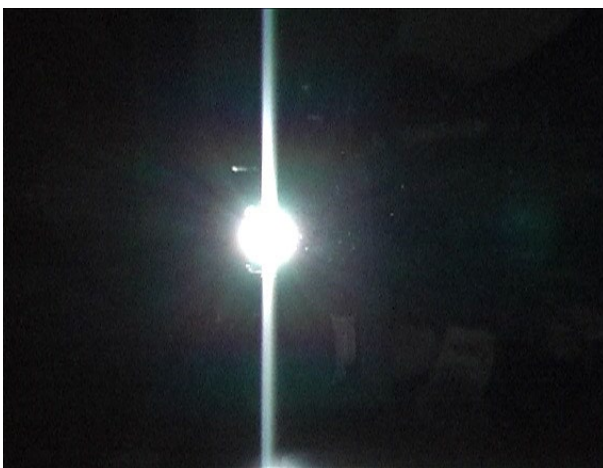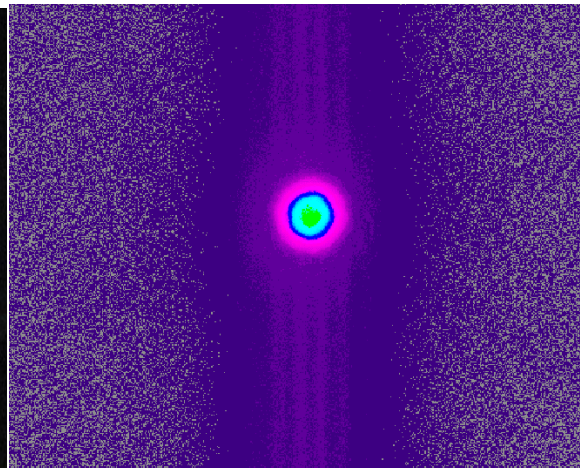

Figure 1. Smearing in CCDs

Figure 2. Smearing in SP920, 1070 nm

This smearing too is absent in CMOS cameras. Some CMOS cameras show a different, less severe, form of beam broadening for NIR light sometimes referred to as blooming. Blooming has been ascribed to the poorly absorbed NIR light bouncing off the back of the silicon wafer in which the CMOS pixel array has been formed and diffracting to the sides.

In a typical CMOS sensor the photodiode pixels and accompanying transistors are fabricated in the top layer of a silicon substrate. On top of this are deposited metal wires to transmit the data for further processing. In the backside illuminated sensor, the silicon is flipped and thinned so that the photodiodes can be illuminated without being shaded by the metal wires. This increases the light collecting efficiency of the photodiode, improving sensitivity.
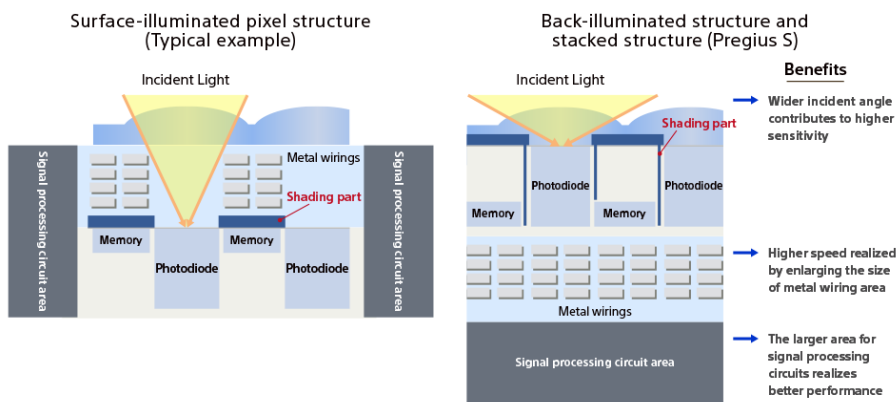

Figure 3. https://www.sony-semicon.com/en/technology/industry/pregius.html

Furthermore, in the latest backside illuminated sensors, the signal processing circuitry is embedded in a separate layer below the sensing layer (instead of in the same layer off to the side). Each of these layers can be optimized for their respective tasks independently, resulting in increased saturation levels and reduced noise. As an additional benefit, in the thinner silicon of the backside illuminated CMOS sensor, the blooming mentioned previously is greatly reduced. Here is a comparison of the blooming in a frontside illuminated sensor and backside illuminated sensor:
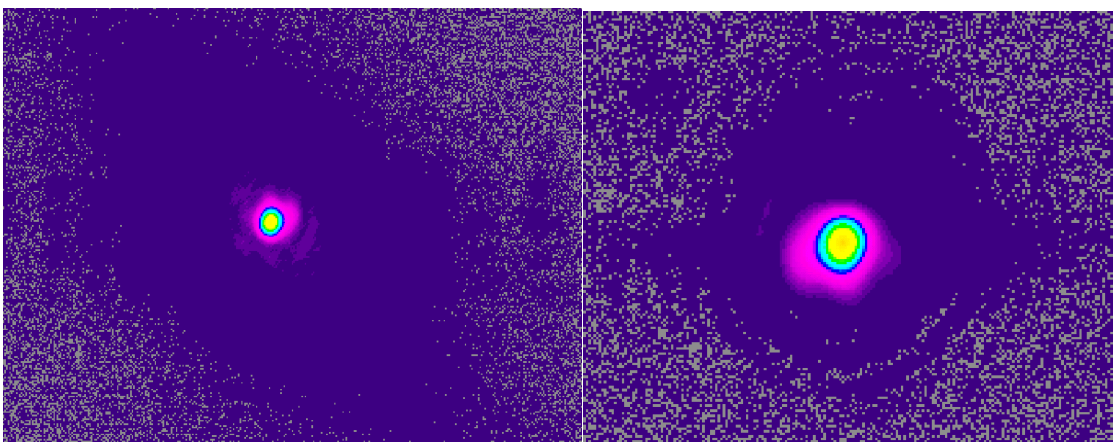
Frontside illuminated sensor   Backside illuminated sensor

Figure 4. 1064 nm laser, 10 ms exposure.

The new camera also has lower temporal dark noise giving it a higher sensitivity threshold and significantly greater dynamic range than our previous cameras.

Camera	SP920	SP932	SP204S
Sensor	CCD	CMOS, frontside ill.	CMOS, backside ill.
EMVA data			
Quantum efficiency at 530 nm [%]	54.62	71.61	73.7
Gain K [DN/e-]	6.9061	5.7837	0.58
Inverse Gain 1/K [e-/DN]	0.1448	0.1729	1.730
Temporal dark noise (read noise) [e-]	12.0473	15.4	2.2
Signal to Noise Ratio SNRmax	95.5324	103.9763	80.1
1/SNRmax [%]	1.0468%	0.9618%	1.2%
Signal to Noise Ratio SNRmax [dB]	39.603	40.3387	38.1
Signal to Noise Ratio SNRmax [bits]	6.5779	6.7	6.3
Absolute sensitivity Threshold μp.min [photons]	22.9715	21.75	3.7
Absolute sensitivity Threshold μe.min [e-]	12.55	15.58	2.7
Saturation Capacity μe.sat [e-]	9126.4	10811	6415
Saturation Capacity μp.sat [photons]	16709	15097	8710
Dynamic Range	727.3562	694.0765	2340
DR [dB]	57.2349	56.8281	67.4
DR [bits]	9.5065	9.439	11.2
DSNU1288 [e-]	5.1395	6.4715	0.3
DSNU1299 [DN]	35.4895	37.4334	0.2
PRNU1288 [%]	0.8304	1.2753	0.4
Linearity error LEmin [%]	-1.254	-0.0823	-0.1
Linearity error LEmax [%]	1.0284	0.3258	0.1
Dark current [e-/sec] , μI.mean			0.15
Camera Temperature [C]	65	58	

Figure 5. Comparison of camera performance properties

BeamSquared and New CMOS SP204S camera

The improvement most relevant for the M^2 measurement brought by the new camera, however, is the smaller pixel size. The SP204S 2.74 um pixels are 61% smaller than those of the SP920 and, thus, can measure smaller focal spots. This ability permits the use of shorter focal length lenses for a given input beam size or allows the measurement of larger beams for a given focusing lens. As alluded to above, the images in the near IR display broadening for moderate spot sizes for short exposure times. The improvement, however, is only felt weakly in the calculated M² parameters since broadening in a few data points is diluted when fitting to the full data set. In a comparison between the measured beam parameters of different lasers using the old and new cameras, there is good agreement (see figure 6).

Other than the waist location (which is known to have a larger relative error) and the M² value for the IR laser, the values agree to within 1 or 2%, well within the specifications.
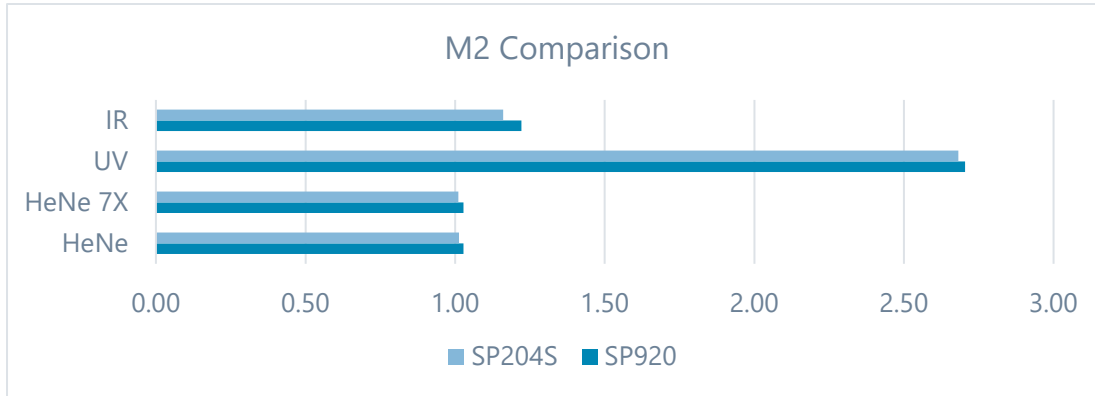
Parameter	Laser	SP920	SP204S	%Change
M-squared	HeNe	1.03	1.01	-1.5%
	HeNe 7X	1.03	1.01	-1.6%
	UV	2.70	2.68	-0.8%
	IR	1.22	1.16	-5.0%
Waist Width (mm) after lens	HeNe	199	197	-0.8%
	HeNe 7X	71.4	71.0	-0.6%
	UV	213	211	-0.9%
	IR	73.8	74.0	0.3%
Waist Location (mm) laser	HeNe	1431	1432	0.0%
	HeNe 7X	1888	1814	-3.9%
	UV	10526	10905	3.6%
	IR	2153	2147	-0.3%
Rayleigh Length (mm) laser	HeNe	370	367	-0.6%
	HeNe 7X	25601	25769	0.7%
	UV	18838	18761	-0.4%
	IR	66.6	67.2	0.8%
Divergence (mrad) laser	HeNe	1.50	1.49	-0.4%
	HeNe 7X	0.180	0.178	-1.1%
	UV	0.264	0.263	-0.6%
	IR	4.99	4.85	-2.8%
BPP (mm mrad) laser	HeNe	0.21	0.20	-1.2%
	HeNe 7X	0.21	0.20	-1.5%
	UV	0.323	0.320	-0.9%
	IR	0.41	0.39	-5.1%

Figure 6. Comparison measurements between the old and new cameras.

In the SP204S, some broadening still occurs for the smallest NIR spots but this will only impact a few of the measurement points in the M² measurement of the largest input beams (above 4 mm diameter when using a 600 mm focal length lens). As previously mentioned, the effect on the derived beam parameters will be minimal.

Repeatability remains good. The standard deviation for successive measurements on a certain camera and for the measurements between different units is low. See figure 7 below. The value derived for the waist location remains the exception. Its standard deviation varied between 4 – 14%. However, when normalized against the Rayleigh length instead of the waist location value itself, the variation becomes relatively small. See figure 8 below.
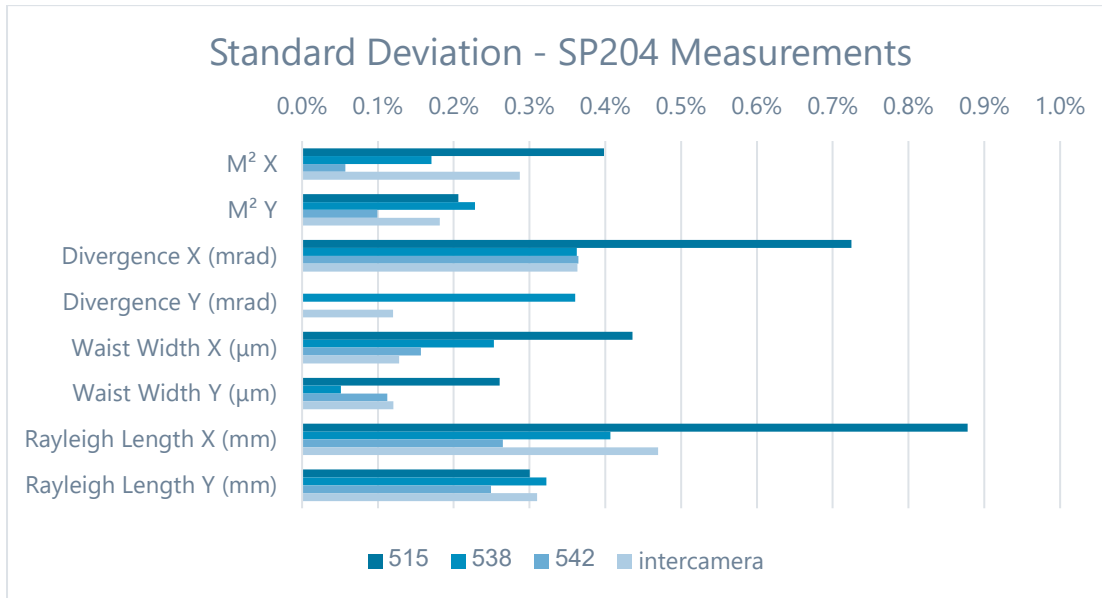

Standard Deviation - SP204 Measurements

Figure 7. Standard deviation in 3 measurements taken with each camera and between the averaged readings of the 3 cameras.

		Waist Location X (mm)	Waist Location Y (mm)
515	Relative to Location	5.0%	-13.7%
	Relative to Rayleigh's length	0.8%	0.7%
538	Relative to Location	4.0%	-7.5%
	Relative to Rayleigh's length	0.6%	0.4%
542	Relative to Location	8.8%	-3.0%
	Relative to Rayleigh's length	1.2%	0.1%
Between cameras	Relative to Location	8.1%	-10.8%
	Relative to Rayleigh's length	1.2%	0.6%

Figure 8. Standard deviation in waist location relative to location value and Rayleigh length.

In summary, the new BeamSquared camera is superior to its predecessor, but its advantages will go largely unnoticed for routine measurements. The new BeamSquared equipped with SP204s camera shows reduced broadening and may give slightly smaller M^2 values for NIR wavelengths.